Supporting Information

Rational Design and Functionalization of a Zn-MOF for highly selective detection of TNP

Shanghua Xing[a], Qiming Bing[b], Hui Qi[c], Jingyao Liu[b], Tianyu Bai[a], Guanghua Li[a], Zhan Shi[a], Shouhua Feng[a], and Ruren Xu[a]*

[a]State Key Laboratory of Inorganic Synthesis and Preparative Chemistry, College of Chemistry, Jilin University, Changchun 130012, P. R. China.

E-mail: leegh@jlu.edu.cn

[b]Institute of Theoretical Chemistry, Jilin University, Changchun, 130023.

[c]The Second Hospital of Jilin University, Changchun 130041, PR China

Contents

Section 1. Experimental section

Materials and methods

All reagents and solvents were obtained commercially and used without further purification. Elemental analyses (C, H, and N) were achieved by vario MICRO (Elementar, Germany). UV/vis spectra were recorded on a UV-2450 UV-visible spectrophotometer within the wavelength range 200–500 nm using the same solvent in the examined solution as a blank. X-ray powder diffraction (PXRD) patterns were taken on a Rigaku D/max 2550 X-ray powder diffractometer. TG analysis was performed on a TGA Q500 V20.10 Build 36. The fluorescence spectra of the samples were recorded on an Edinburgh Instruments FLS920 spectrofluorimeter equipped with both continuous (450 W) and pulsed xenon lamps.

X-ray crystallography

The data collection and structural analysis of crystal was performed on a Rigaku RAXIS-RAPID equipped with a narrow-focus, 5.4 kW sealed tube X-ray source (graphite-monochromated Mo-Ka radiation, λ = 0.71073 Å) at 293 K. The data processing was accomplished with the PROCESS-AUTO processing program. Direct methods were used to solve the structure using the SHELXL crystallographic software package[1-2]. All non-hydrogen atoms were easily found from the difference Fourier map. All non-hydrogen atoms were refined anisotropically. The guest molecules can be calculated from the TGA and elemental analyses (C, H and N). The crystal data, data collection, and refinement parameters for compound are listed in Table S1. Crystallographic data for the structure have been deposited with Cambridge Crystallographic Data Centre with CCDC Number: 1520296-1520297. Full experimental details and crystallographic analysis are given in the ESI.

Theoretical calculations

First-principles spin-polarized density functional theory (DFT) calculations were performed using the Vienna Ab initio Simulation Package (VASP)[3]. The projector augmented wave (PAW) potentials[4-5], and the Perdew-Burke-Ernzerhof (PBE) functional[6] were used to describe the

electron-ion interactions and the nonlocal exchange correlation energy, respectively. Long-range dispersion corrections have been taken into consideration within the DFT-D2 approach of Grimme[7], which is implemented in the latest version of VASP.

The theoretically optimized model of compound 1 was constructed based on the single crystal data. The compound 2 model was built based on the optimized structure of compound 1 by replacing the hydrogen atom with amino group. The unit cell of compound 2 or 1 was adopted as the repeated structural unit with one 2,4,6-trinitrophenol (TNP) molecule adsorbed in the channel of each unit. A cutoff energy of 400 eV was used for the plane-wave expansion and the Brillouin zone was sampled with a (1×3×3) Monkhorst-Pack k-point grid. The geometry optimization was stopped when the force on each atom was less than 0.02 eV/Å.

Fluorescence Quenching Titration

The fluorescence properties of activated compound 1or 2 were investigated in DMF suspension at room temperature. The stock suspension was prepared by dispersing activated compound 1or 2 (2 mg) in DMF (2 mL), and then sonicated for 30 min. The fluorescence response in 400-550 nm range upon excitation at 360 nm was measured in-situ after incremental addition of freshly prepared DMF analyte solutions (1 mM). The solution was stirred at constant rate during fluorescence measurement and maintains homogeneity of solution. Each titration was repeated at least three times to obtain reliable data.

Section 2. Structure Information

Table S1. Crystallographic data and structural refinement details for compound 1 and 2.

Compound	1	2
Formular	$C_{51}H_{59}N_6O_{20}Zn_4$	$C_{51}H_{59.5}N_{6.5}O_{20}Zn_4$
Formula weight	1337.52	1345.03
Crystal system	Monoclinic	Monoclinic
Space group	$P2_1/n$	$P2_1/n$
a (Å)	10.313(2)	10.304(2)
b (Å)	27.814(6)	27.768(6)
c (Å)	26.011(5)	26.268(5)
β (^{o})	92.25(3)	92.44(3)
V (Å^3)	7455(3)	7509(3)
Z	4	4
dcalc, g cm^{-3}	1.192	1.190
Reflections	64795 / 16352	65249 / 16428
Collected/unique	[R_{int} = 0.1423]	[R_{int} = 0.0572]
Data/restraints/parameters	16352 / 14 / 487	16428 / 18 / 499
Final R indices [$I > 2\sigma(I)$][a,b]	R_1 = 0.0590, wR_2 = 0.1304	R_1 =0.0525, wR_2 = 0.1430
R indices (all data)	R_1 = 0.1250, wR_2 = 0.1453	R_1 = 0.0713, wR_2 =0.1505
Gof	0.936	1.056

[a] $R_1 = \Sigma||F_o| - |F_c||/\Sigma|F_o|$, [b] $wR_2 = [\Sigma w(|F_o|^2 - |F_c|^2)/\Sigma|w(F_o^2)^2|]^{1/2}$

Section 3. Basic characterization experiments

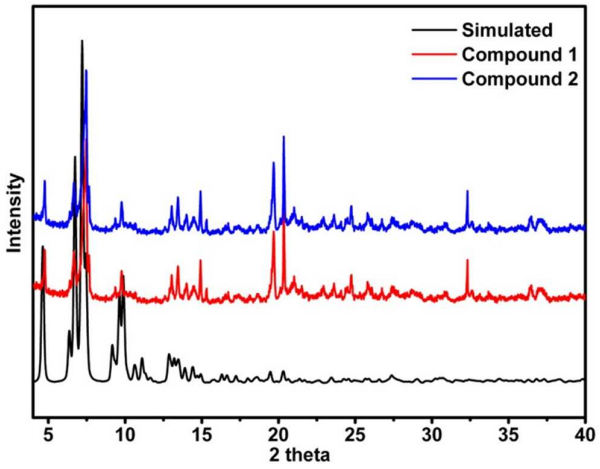

Fig. S1 Powder XRD patterns for simulated, as-synthesized compound 1 and 2.

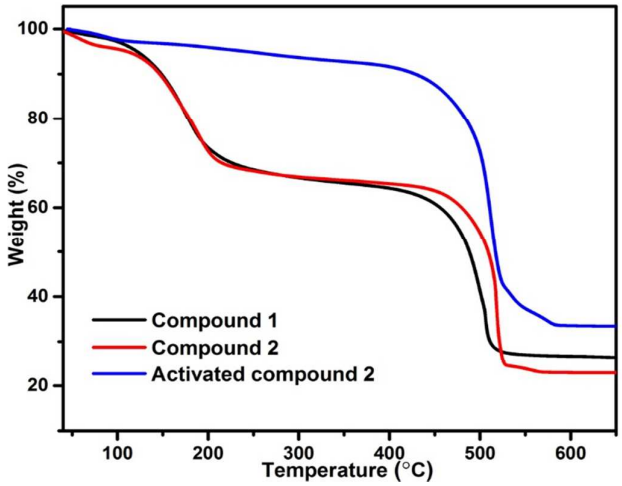

Fig. S2 Thermogravimetric analysis curves of as-synthesized compound 1 and 2.

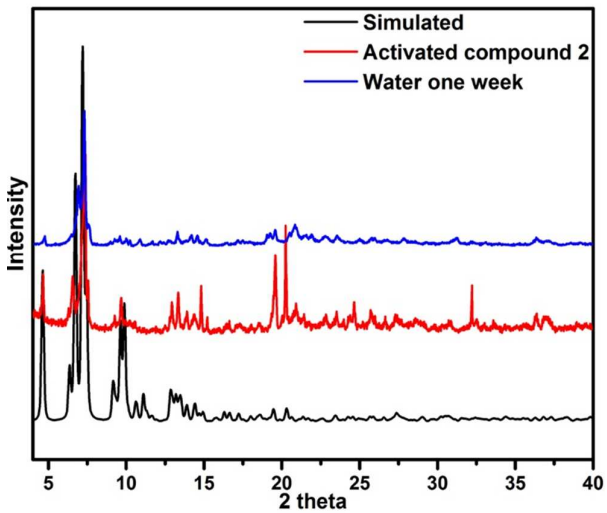

Fig. S3 Powder XRD patterns for simulated, activated and immersed in water one week of compound 2.

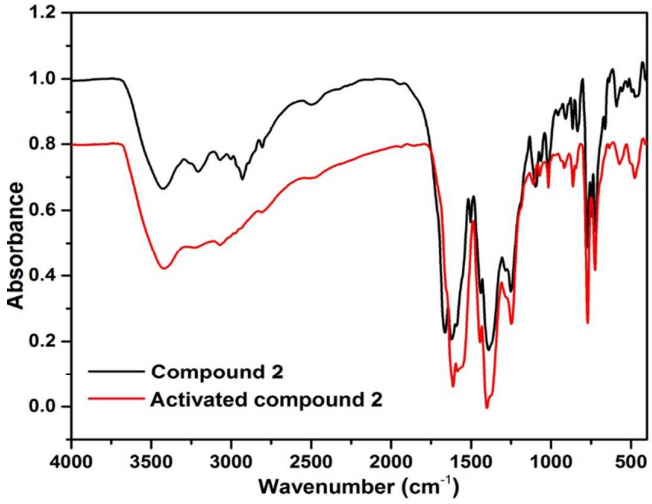

Fig. S4 FT-IR spectra of compound 2 and activated compound 2.

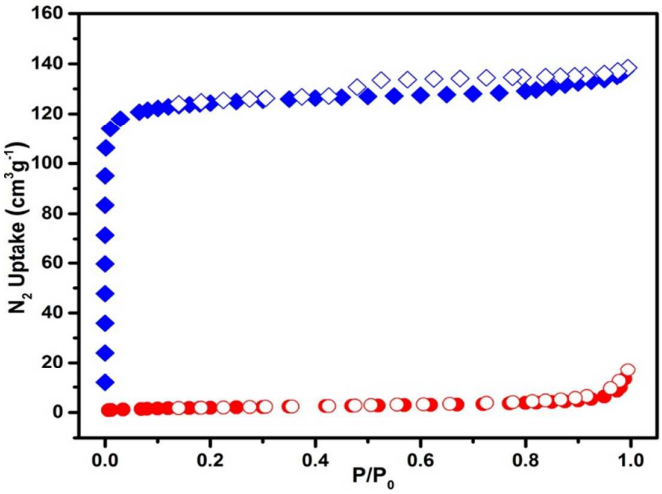

Fig. S5 N_2 adsorption isotherm of compound 2 before and after sensing TNP

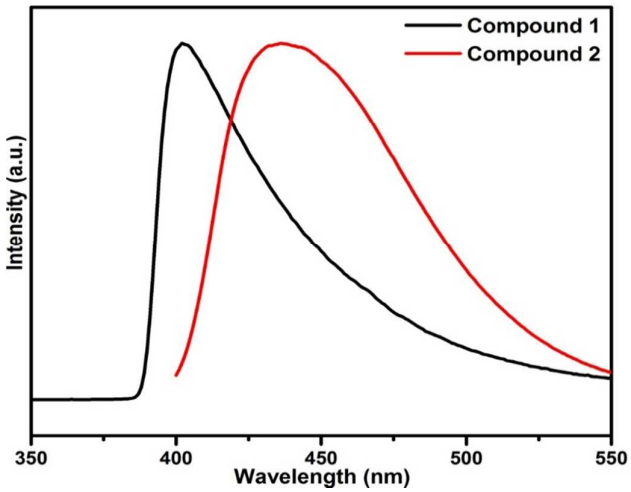

Fig. S6 The Solid-state emission spectra of compound 1 and 2

Section 4. Detection of TNP and other nitro explosives

Table S2. Comparison of detection capacities of compound 2 towards TNP with other materials.

MOF	K_{sv} (M^{-1})	Detection limit	Ref.
$[Cu(L)(I)]_{2n}\cdot 2nDMF\cdot nMeCN$	2.9×10^4	0.0066 mM	8
$[Zn_2(L)_2(dpyb)]$	2.4×10^4		9
$[Zn(L)(dipb)](H_2O)_2$	2.46×10^4		9
$[Zn_2(TPOM)(NH_2\text{–}BDC)_2]\cdot 4H_2O$	4.6×10^4	9.8×10^{-7} M	10
$[Cd_5Cl_6(L)(HL)_2]\cdot 7H_2O$	4.05×10^4	1.87×10^{-7} M	11
$Zn_2(TZBPDC)(\mu_3\text{-}OH)(H_2O)_2$	4.9×10^4	2.78×10^{-7} M	12
$[(Zn_4O)(DCPB)_3]\cdot 11DMF\cdot 5H_2O$	3.7×10^4		13
$[Cd(NDC)_{0.5}(PCA)]\cdot Gx$	3.5×10^4		14
$Zr_6O_4(OH)_4(L)_6$	2.9×10^4		15
$[(CH_3)_2NH_2]_3[Zn_4Na(BPTC)_3]$	3.2×10^4		16
$[Eu_3(bpydb)_3(HCOO)(\mu_3\text{-}OH)_2(DMF)]$	2.1×10^4		17
$[Zn_8(ad)_4(BPDC)_6O\cdot 2\ Me_2NH_2]$	4.6×10^4	1.29×10^{-8} M	18
$[Cd_4(L)_2(L_2)_3(H_2O)_2]$	3.89×10^4	1.98 ppm	19

Detection Limit Calculation:

To calculate the standard deviation and detection limit of this detection method, **compound 2** with fine particles was made into a 1mg/mL suspension. Then, TNP solution (1-20 μL, 1mM) was added into the suspension and the fluorescent intensities were recorded. Standard deviation (σ) was calculated from five blank tests of **compound 2** suspension and the detection limit was calculated via the formula: 3σ/m (m: the slope of the linear region).

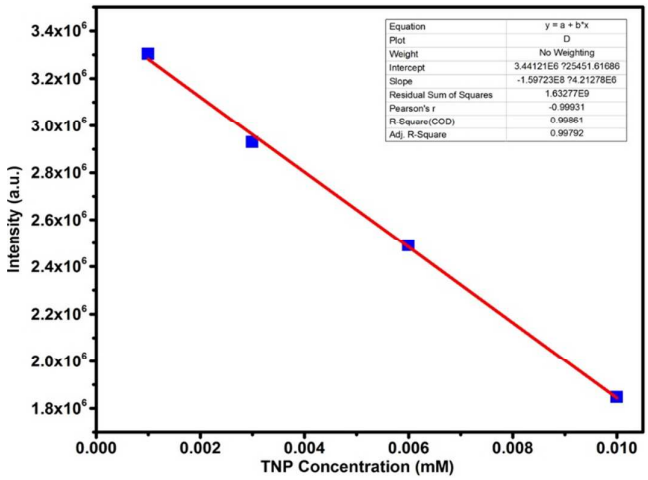

Fig. S7 Linear region of fluorescence intensity of **compound 2** suspension (λex = 360 nm) upon incremental addition of TNP (1 mM).

Table S3. Standard deviation calculation.

	Fluorescence intensity
Text 1	3.56×10^6
Text 2	3.44×10^6
Text 3	3.67×10^6
Text 4	3.66×10^6
Text 5	3.49×10^6
Standard deviation (σ)	88741

Table S4. Detection limit calculation.

Slope (m)	1.597×10^8 mM^{-1}
Detection limit (3σ/m)	0.00056 mM

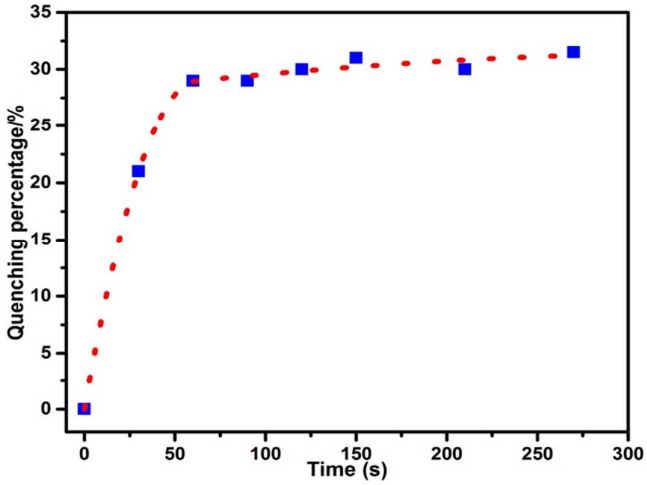

Fig. S8 Time-dependent fluorescence quenching percentage by TNP vapor.

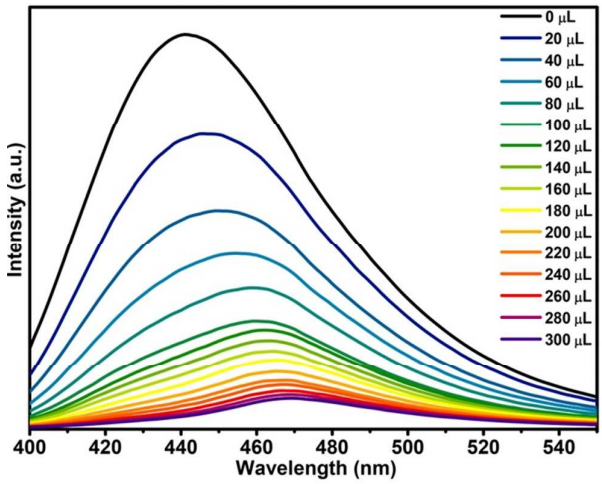

Fig. S9 Effect on the emission spectra of compound 2 dispersed in DMF upon incremental addition of a TNP solution.

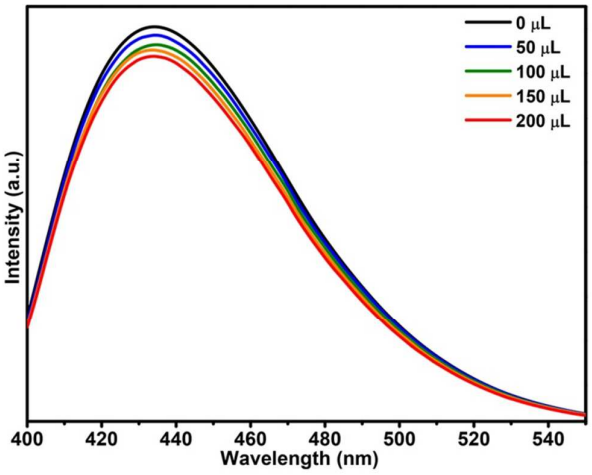

Fig. S10 Emission spectra of compound 2 dispersed in DMF upon incremental addition of 1,3-DNB solution (1mM) in DMF.

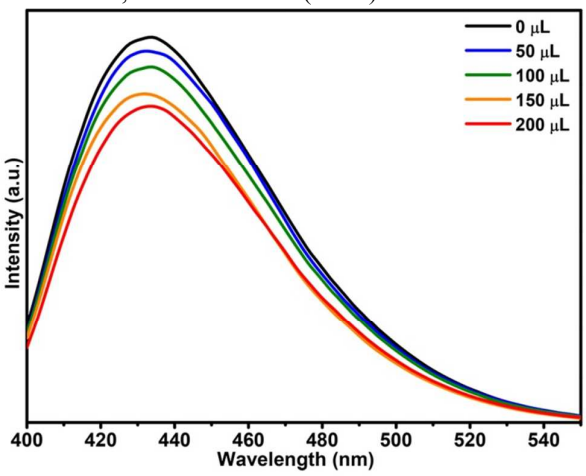

Fig. S11 Emission spectra of compound 2 dispersed in DMF upon incremental addition of 2,4-DNT solution (1mM) in DMF.

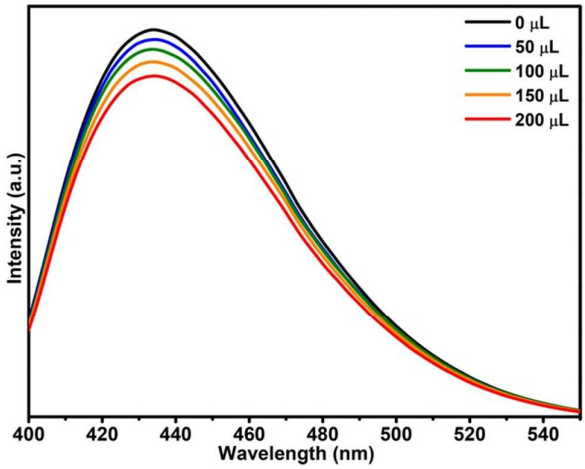

Fig. S12 Emission spectra of compound 2 dispersed in DMF upon incremental addition of 2,6-DNT solution (1mM) in DMF.

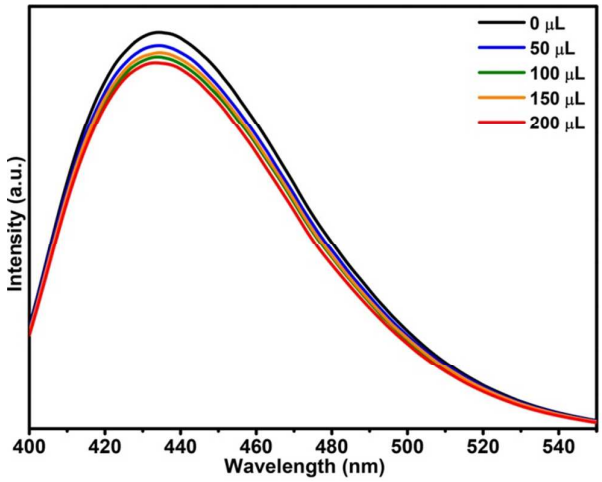

Fig. S13 Emission spectra of compound 2 dispersed in DMF upon incremental addition of NB solution (1mM) in DMF.

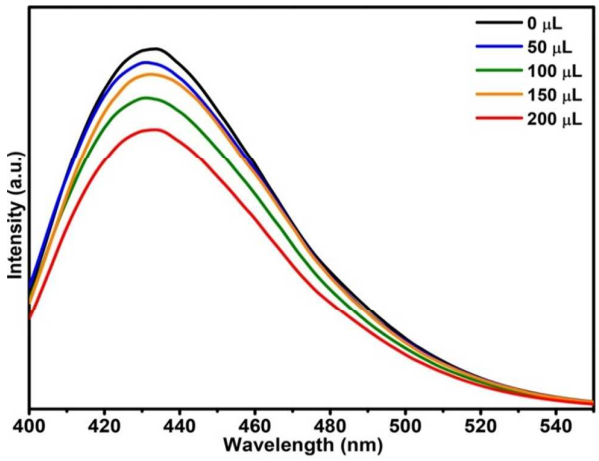

Fig. S14 Emission spectra of compound 2 dispersed in DMF upon incremental addition of NT solution (1mM) in DMF.

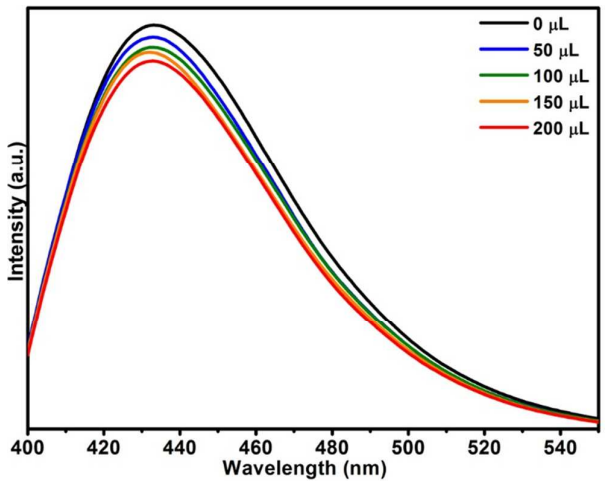

Fig. S15 Emission spectra of compound 2 dispersed in DMF upon incremental addition of NM solution (1mM) in DMF

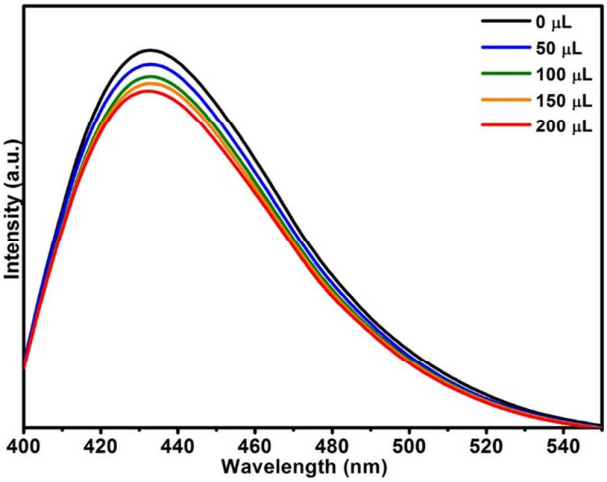

Fig. S16 Emission spectra of compound 2 dispersed in DMF upon incremental addition of NE solution (1mM) in DMF

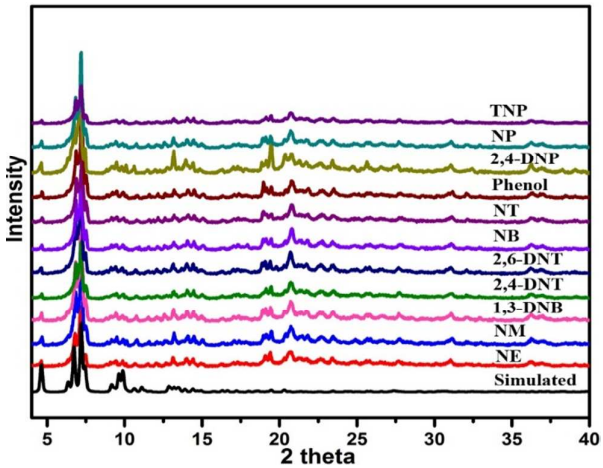

Fig. S17 PXRD patterns of compound 2 treated by various analytes DMF solutions.

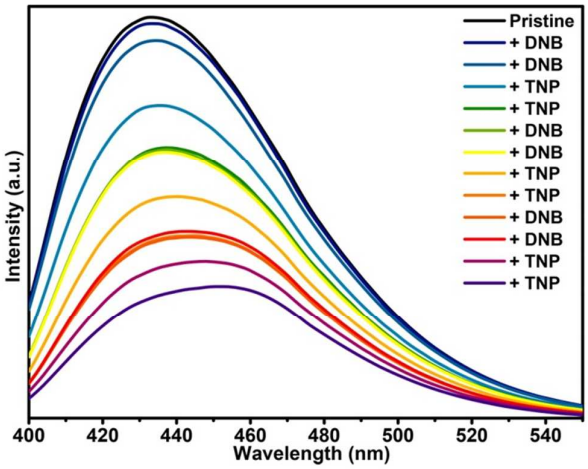

Fig. S18 Emission spectrum of compound 2 upon addition of DMF solution of 1,3-DNB followed by TNP (20µl addition each time).

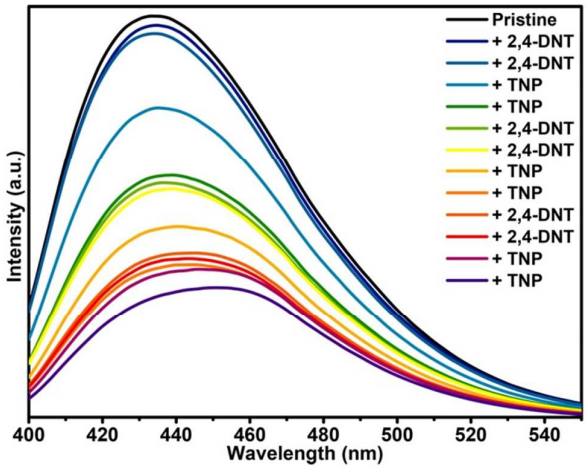

Fig. S19 Emission spectrum of compound 2 upon addition of DMF solution of 2,4-DNT followed by TNP (20µl addition each time).

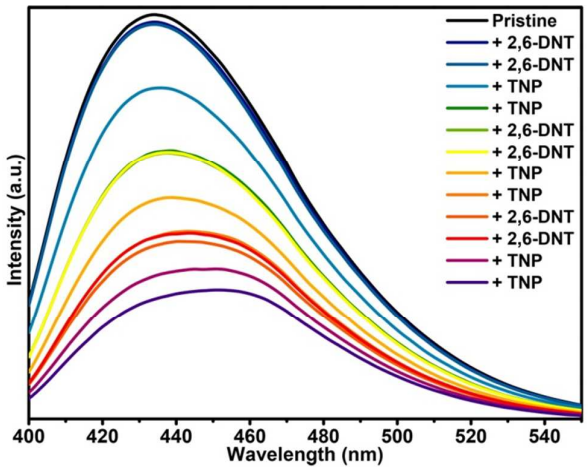

Fig. S20 Emission spectrum of compound 2 upon addition of DMF solution of 2,6-DNT followed by TNP (20µl addition each time).

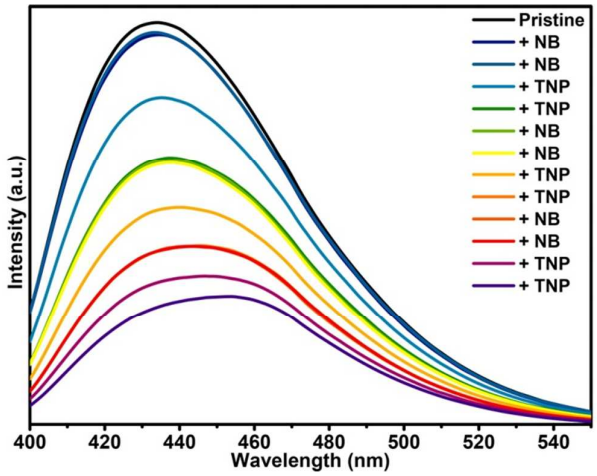

Fig. S21 Emission spectrum of compound 2 upon addition of DMF solution of NB followed by TNP (20µl addition each time).

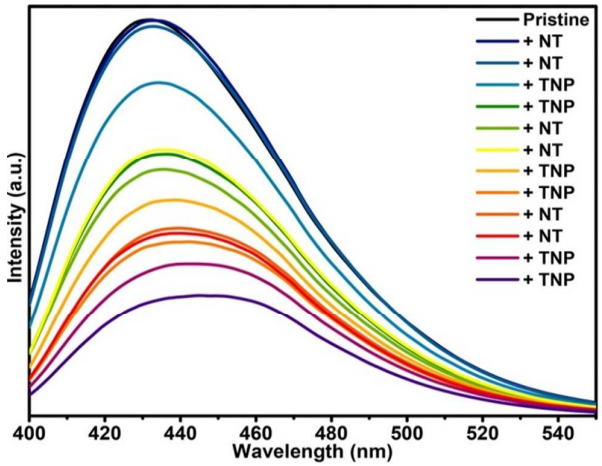

Fig. S22 Emission spectrum of compound 2 upon addition of DMF solution of NT followed by TNP (20µl addition each time).

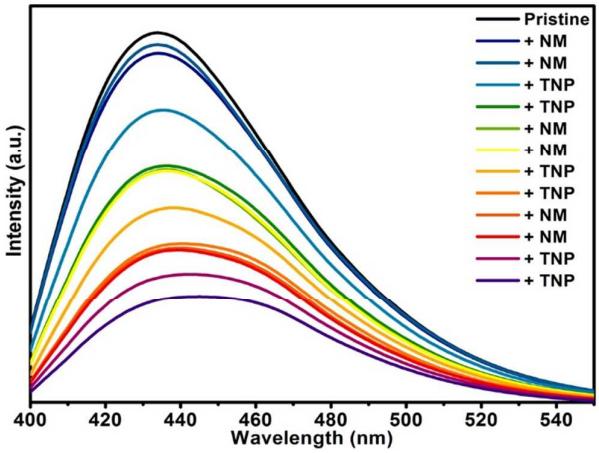

Fig. S23 Emission spectrum of compound 2 upon addition of DMF solution of NM followed by TNP (20µl addition each time).

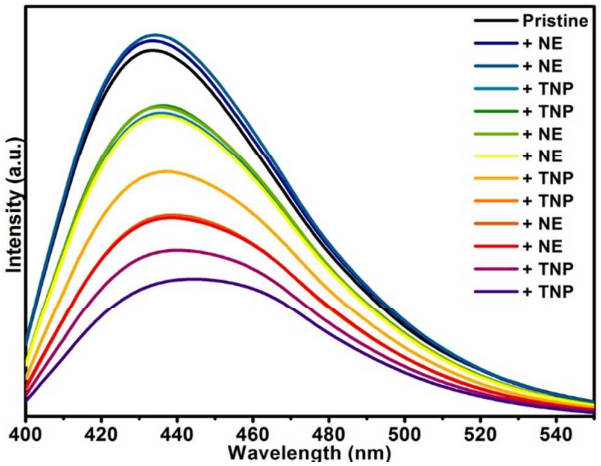

Fig. S24 Emission spectrum of compound 2 upon addition of DMF solution of NE followed by TNP (20µl addition each time).

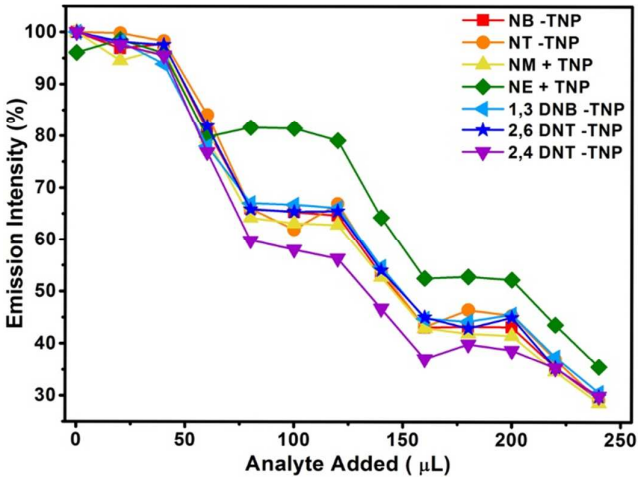

Fig. S25 Decrease in percentage of fluorescence intensity upon the addition of DMF solutions of different nitro compounds followed by TNP.

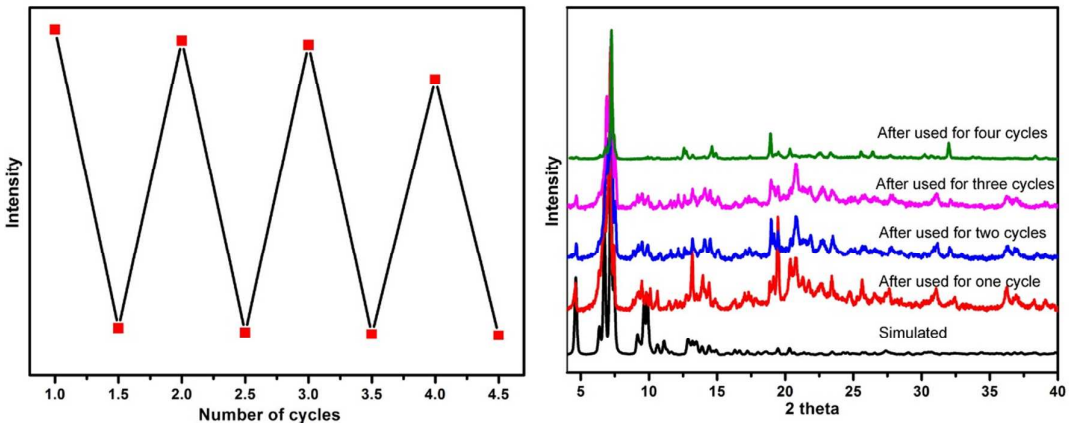

Fig. S26 The changes of emission intensity of four recycles (Left) and PXRD patterns of compound 2 after four recycles (Right).

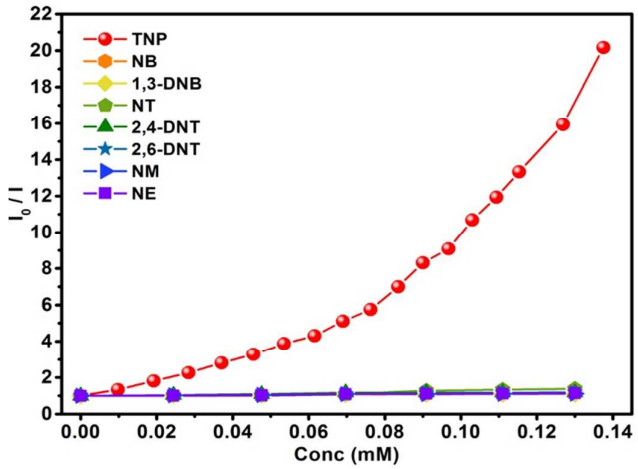

Fig. S27 Stern–Volmer plot for various nitro analytes.

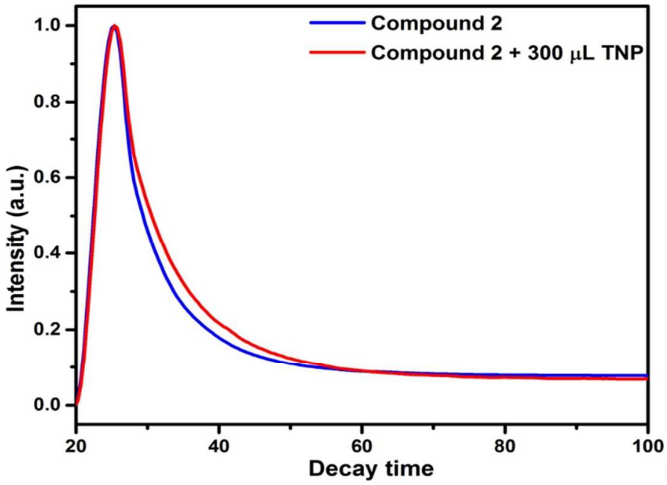

Fig. S28 The decay time of compound 2 before and after adding TNP.

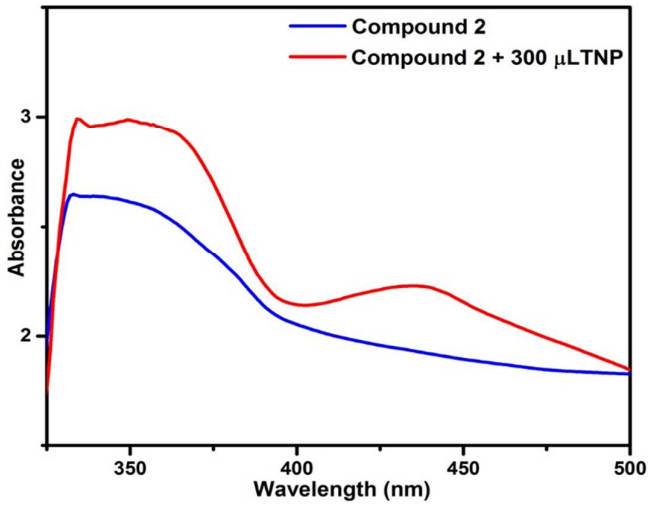

Fig. S29 UV-vis spectra of compound 2 upon gradual addition of TNP showing spectral change with the appearance of new band at 430 nm

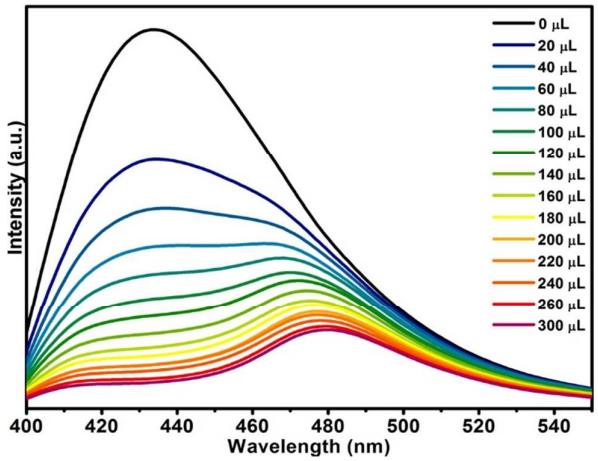

Fig. S30 Emission spectra of compound 2 dispersed in DMF upon incremental addition of 2,4-DNP solution (1mM) in DMF.

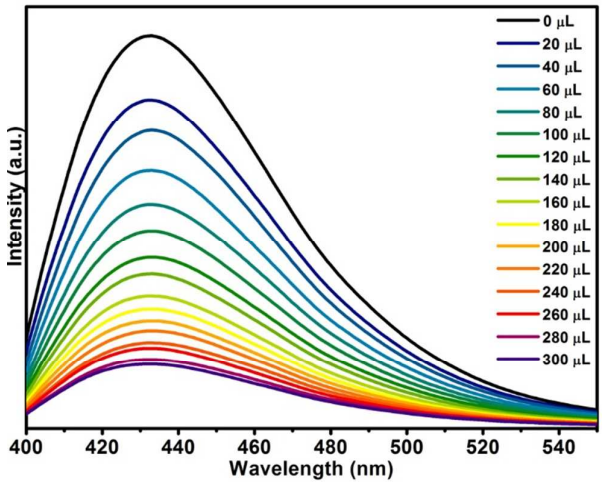

Fig. S31 Emission spectra of compound 2 dispersed in DMF upon incremental addition of NP solution (1mM) in DMF.

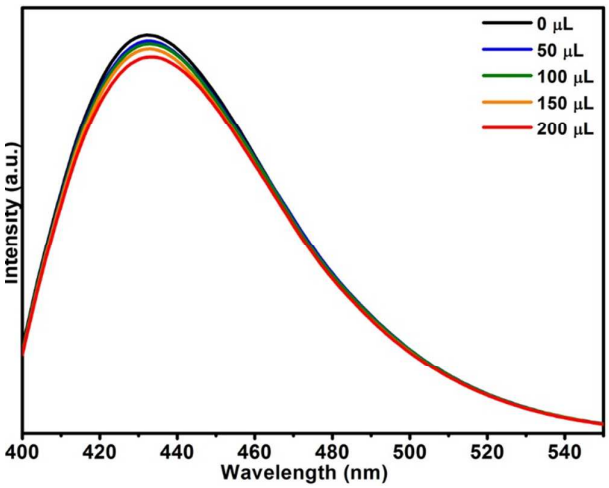

Fig. S32 Emission spectra of compound 2 dispersed in DMF upon incremental addition of phenol solution (1mM) in DMF.

Table S5 HOMO and LUMO energies of the investigated nitro analytes. The data are based on the reported results[20].

Analytes	HOMO (ev)	LUMO (eV)
TNP	-8.237	-3.897
1,3-DMB	-7.985	-3.431
2,4-DNT	-7.764	-3.217
2,6-DNT	-7.644	-3.287
NB	-7.591	-2.428
NT	-7.555	-2.747
NM	-8.508	-2.486
NE	-8.396	-2.331
2,4- DNP	-7.628	-3.325
NP	-6.921	-2.393
Phenol	-6.134	-0.482

References

1. Sheldrick, G. M. SHELXTL Version 5.1 Software Reference Manual, Bruker AXS. Inc. Madison, WI, 1997.

2. Sheldrick, G. M. A Short History of SHELX. Acta Crystallogr. 2008, A64, 112-122.

3. Kresse, G., Furthmuller J. Efficient Iterative Schemes for Ab Initio Total-energy Calculations Using a Plane-wave Basis Set. Phys. Rev. B. 1996, 54, 11169.

4. Blochl, P. E. Projector Augmented-wave Method. Phys. Rev. B. 1994, 50, 17953.

5. Kresse, G.; Joubert, D. From Ultrasoft Pseudopotentials to the Projector Augmented-wave Method. Phys. Rev. B. 1999, 59, 1758.

6. Perdew, J. P.; Burke, K.; Ernzerhof, M. Generalized Gradient Approximation Made Simple Phys. Rev. Lett. 1996, 77, 3865.

7.Shishkin, M.; Kresse, G. Implementation and Performance of the Frequency-Dependent GW Method within the PAW Framework. Phys. Rev. B. 2006, 74, 035101.

8. Khatua, S.; Goswami, S.; Biswas, S.; Tomar, K.; Jena, H. S.; Konar, S.; Stable Multiresponsive Luminescent MOF for Colorimetric Detection of Small Molecules in Selective and Reversible Manner. *Chem. Mater.* **2015**, *27,* 5349-5360.

9. Shi, Z. Q.; Guo, Z. J.; Zheng, H.G. Two Luminescent Zn(II) Metal–organic Frameworks for Exceptionally Selective Detection of Picric Acid Explosives. *Chem. Commun.* **2015**, *51*, 8300-8303.

10. Lv, Rui.; Wang, J. Y.; Zhang,Y. P.; Li, H.; Yang, L. Y.; Liao, S. Y.; Gu, W.; Liu, X. An amino-decorated dual-functional metal–organic framework for highly selective sensing of Cr(iii) and Cr(vi) ions and detection of nitroaromatic explosives. *J. Mater. Chem. A*. **2016**, *4*, 15494-15500.

11.Buragohain, A.; Yousufuddin, M.; Sarma, M. Biswas, S. 3D Luminescent Amide-Functionalized Cadmium Tetrazolate Framework for Selective Detection of 2,4,6-Trinitrophenol. *Cryst. Growth Des.* **2016**, 16, 842−851.

12.Hu, Y. L.; Ding,M. L.; Liu, X. Q.; Bing, S. L.; Jiang, H. L. Rational synthesis of an exceptionally stable Zn(II) metal-organic framework for the highly selective and sensitive

detection of picric acid. *Chem. Commun.* **2016**, *52*, 5734-5737.
13. He, H. M.; Song, Y. Sun, F. X.; Bian, Z.; Gao, L. X.; Zhu, G. S. A porous metal–organic framework formed by a V-shaped ligand and Zn(ii) ion with highly selective sensing for nitroaromatic explosives. *J. Mater. Chem. A.* **2015**, 3, 16598-16603.
14. Nagarkar, S. S.; Joarder, B.; Chaudhari, A. K.; Mukherjee, S.; Ghosh, S. K. Highly selective detection of nitro explosives by a luminescent metal-organic framework. *Angew. Chem. Int. Ed.* **2013**, *52*, 2881–2885.
15. NAGARKAR S S, DESAI A V and GHOSH S K. A fluorescent metal-organic framework for highly selective detection of nitro explosives in the aqueous phase. *Chem Commun*. **2014**, *50*, 8915-8918.
16. Zhou, E. L.; Huang, P.; Qin, C.; Shao, K. Z.; Su, Z. M. A stable luminescent anionic porous metal–organic framework for moderate adsorption of CO_2 and selective detection of nitro explosives. *J. Mater. Chem. A,* **2015**, *3*, 7224-7228.
17. Song, X. Z.; Song, S. Y.; Zhao, S. N.; Hao, Z. M.; Zhu, M.; Meng, X.; Wu, L. L.; Zhang, H. J.Single-Crystal-to-Single-Crystal Transformation of a Europium(III) Metal-Organic Framework Producing a Multi-responsive Luminescent Sensor. *Adv. Funct. Mater*. **2014**, *24*, 4034-4041.
18.Joarder, B.; Desai, A. V.; Samanta, P.; Mukherjee, S.; Ghosh, S. K. Selective and sensitive aqueous-phase detection of 2,4,6-trinitrophenol (TNP) by an amine-functionalized metal-organic framework. *Chem. Eur. J.* 2**015**, *21*, 965-969.
19. Pal, T. K.; Chatterjee, N.; Bharadwaj, P. K. Linker-Induced Structural Diversity and Photophysical Property of MOFs for Selective and Sensitive Detection of Nitroaromatics. *Inorg Chem*, **2016**, *55*, 1741-1747.
20. Frisch, M. J.; Trucks, G. W.; Schlegel, H. B. Scuseria, G. E.; Robb, M. A.; Cheeseman, J. R.; Scalmani, G.; Barone, V.; Mennucci, B.; Petersson, G. A.; Nakatsuji, H.; Caricato, M.; Li, X.; Hratchian, H. P.; Izmaylov, A. F.; Bloino, J.; Zheng, G.; J. Sonnenberg, L.; Hada, M.; Ehara, M.; Toyota, K.; Fukuda, R.; Hasegawa, J.; Ishida, M.; Nakajima, T.; Honda,Y.; Kitao, O.; Nakai, H.; Vreven, T.; Montgomery, J. J. A.; Peralta, J. E.; Ogliaro, F.; Bearpark, M.; Heyd, J. J.; Brothers, E.; Kudin, K. N.; Staroverov, V. N.; Keith, T.; Kobayashi, R.; Normand, J.; Raghavachari, K.; Rendell, A.; Burant, J. C.; Iyengar, S. S.; Tomasi, J.; Cossi, M.; Rega, N.; Millam, J. M.; Klene, M.; Knox, J. E.; Cross, J. B.; Bakken, V.; Adamo, C.; Jaramillo, J.; Gomperts, R.; Stratmann, R. E.; Yazyev, O.; Austin, A. J.; Cammi, R.; Pomelli, C.; Ochterski, J. W.; Martin, R. L.; Morokuma, K.; Zakrzewski,V. G.; Voth, G. A.; Salvador, P.; Dannenberg, J. J.; Dapprich, S.; Daniels, A. D.; Farkas, O.; Foresman, J. B.; Ortiz, J. V.; Cioslowski, J.; Fox, D. J. Gaussian 09, Revision C.01, Gaussian, Inc., Wallingford, CT, **2010**.